2DH modelling of a reservoir flushing compared with LSPIV measurements

B. Camenen, André Paquier, A. Bouarab, J. Le Coz, Guillaume Dramais, M. de Linares

2DH modelling of a reservoir flushing compared with LSPIV measurements

B. Camenen[1], A. Paquier[1], A. Bouarab[1], J. Le Coz[1], G. Dramais[1], M. De Linares[2]
[1]Cemagref, UR HHLY, 3 bis quai Chauveau, CP 220,
F-69336 Lyon cedex 09, FRANCE
[2]Sogreah, 6, rue de Lorraine, BP 218,
F-38432 Echirolles cedex, FRANCE
Email: andre.paquier@cemagref.fr

Abstract: *A reservoir flushing was completed on September 2008 in the Longefan reservoir (Arc en Maurienne River, France). This reservoir (approximately 300m×500m) is part of the EDF (French Electricity company) hydropower system. It is mainly used for the sedimentation of the water released from the upstream hydropower plant and for temporary storage for the next plant. LSPIV measurements were completed during the flushing event using three cameras covering the main zones of interest (entrance, main channel and exit). For each movie, biologically degradable chips were injected to produce visible patterns on the surface flow and facilitate the LSPIV processing. Two 2DH hydrodynamic models (Rubar20and Telemac2D) were applied to the system and their results were compared to the experimental data. Advantages and limits of these models were discussed. In particular, the effects of water level and wind were studied as well as the direction of the jet entering the reservoir.*

Keywords: *reservoir hydraulics, flushing event, LSPIV, numerical modelling.*

1. INTRODUCTION

All reservoirs formed by dams on natural rivers are subject to some degree of sediment inflow and deposition. Because of the very low velocities in reservoirs, they tend to be very efficient sediment traps. Therefore, the amount of reservoir sedimentation over the lifetime of the project needs to be predicted before the project is built (Yang, 2006). Reservoir sedimentation is a serious problem in many regions with high sediment yield. In order to maintain some capacity of the reservoir, new methodologies of management need to be tested. Flushing is generally used to reduce or balance sediment accumulation and to recover reservoir capacity, and has been successfully applied to numerous hydropower and irrigation reservoirs (Morris and Fan, 1998). However, for large reservoirs, the efficiency of flushing operations may be poor.

The Longefan reservoir is located next to the Arc River in the French Alps. The Arc catchment is approximately 2000km2 and shows a very high sediment yield. Concentrations up to 30g/l may be observed during flood event and even larger when a debris flow occurred in a tributary (Camenen et al., 2008). The Longefan reservoir is part of a complex system managed by EDF to optimize hydro-electricity production. It has two utilities: (a) as a sedimentation reservoir for the water coming from the Hermillon hydropower plant, and (b) as a capacitive reservoir for the Cheylas hydropower plant (through the Flumet reservoir, which is connected to the Longefan reservoir with a gallery). It is approximately 500m long and 300m large (see also Fig. 2), and so has a capacity of 1.5 million m3. However, this capacity was reduced by 40% due to large sedimentation occurring in the reservoir. For this main reason, some new solutions were tested by EDF to reduce this sedimentation and optimize the capacity of the Longefan reservoir. A first test was a flush carried out on September 25th and 26th, 2008. In order to better understand erosion and deposition dynamics in the reservoir, measurements of the velocities and suspended load concentrations were carried out during the event as well as bathymetric survey before and after the event.

This work is part of the project “Sustainable Management of Sediment for the hydroelectric scheme of Arc-Isère” set up by EDF (Electricity of France) to address productivity losses due to high sedimentation in the reservoirs. This sediment management approach in reservoirs addresses sedimentary, environmental, and operating factors. The goal is to define a sustainable strategy that will addresses all aspects of sediment management including economics, production, environmental and regulatory constraints.

2. EXPERIMENTAL SET-UP

2.1. Flushing event of September 25th and 26th, 2008

The program of the reservoir flush is presented on Fig. 1. Starting from an empty reservoir, the gate for the gallery connected to the Flumet reservoir being closed, a varying input discharge was obtained using one or two turbines from the hydropower plant, whereas the output discharge was regulated thanks to another gate. The flushing event lasted approximately 40 hours.
On Fig.1, one can observe the evolution of the water level measured next to the entrance of the reservoir together with the input and output discharges (denoted Q_{in} and Q_{out}, respectively). If the input discharge could be estimated accurately from the output power of turbines as it corresponds to turbinated water, there are some large uncertainties on the output discharge, which was estimated from a gate hydraulic law. Actually, one can easily observe some errors for this discharge estimation as the water level often varies even if Q_{out} was estimated equal to Q_{in} (the discharge in the circular spillway was set to zero).

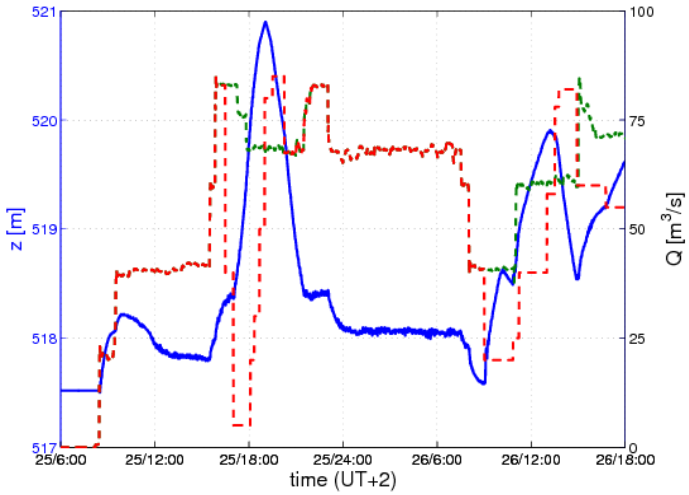

Figure 1 Water level (NGF) in the Longefan reservoir (blue solid line) associated with input discharge (red dashed line) and output discharge (green dashed line).

2.2. LSPIV measurements

Since the seminal work of Fujita et al. (1998), the application of the Particle Image Velocimetry (PIV) technique to large-scale parts of free-surface field flows has been disseminated widely and successfully in the hydraulic research and engineering community (Muste et al., 2008). In this paper, we attempt to apply the Large Scale PIV (LSPIV) to estimate the surface velocities in the Longefan reservoir during the flushing event.
In Fig.2, a schematic view of the Longefan reservoir is presented with the position of three cameras deployed around the reservoir together with the approximate view scope of the cameras. Three commercial cameras were used (one Canon 750i and two Panasonic HDC-HS9). The water colour was very dark due to high concentrations of fine suspended sediment. White artificial tracers (Ecofoam chips, a biodegradable, water soluble foam filled material; see Jodeau et al., 2008) contrasting in colour with the water free-surface were used to improve the detection of flow movement. However, as seeding was possible only at the entrance in the reservoir, tracers were visible from camera 1 only. For the camera 2 and 3, the processing of the images has been possible using surface patterns due to local variations of the concentration.
The orthorectification of the images was achieved thanks to GRP's (Ground reference Point) positioned on the parapet around the reservoir or on the two large deposits in the reservoir. For all the cameras, 8 to 13 GRP's could be observed on the image within both near and far fields.
Several movies have been recorded and processed using the LSPIV method with Δt = 1s between two successive images (Muste et al., 2008 ; Jodeau et al., 2008). For camera 1, the orthopixel resolution was generally set to r = 0.01 (1 pixel = 1 cm) and the minimum correlation between two images Cor = 0.4: the image field was close and the patterns (chips) clear. On the other hand, for cameras 2 and 3,

the image field was distant and the patterns (water colour) blurry: r = 0.1 and Cor = 0.1 were chosen. Tab. 1 gives approximately the time (UT+2) of the LSPIV sequences together with the water level of the reservoir (measured close to the entrance).

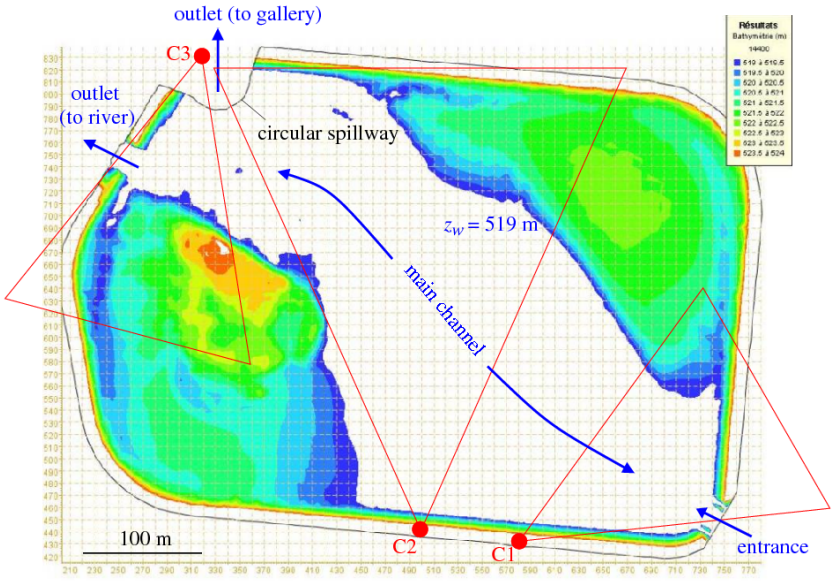

Figure 2 Position of the cameras around the Longefan reservoir.

Table 1 Summary table of the LSPIV sequences.

Date	Time (UT+2)	Water level	Camera 1	Camera 2	Camera 3
25/09/2008	09:00-10:30	518.0m	09:25	09:00	-
		518.2m	-	09:45	10:25
	10:30-13:00	518.1m	-	-	11:20
	13:00-15:00	517.8m	-	14:10	-
	15:00-17:00	518.2m	15:35	16:20	16:50
	17:00-19:00	520.9m	19:00		
26/09/2008	09:00-10:30	518.3m	09:35	09:35	09:45
	10:30-13:30	519.5 m	12:50	11:45	13:05
	13:30-15:00	519.1 m	14:55	13:50	-
	15:00-17:00	518.8m	-	-	15:15

3. RESULTS

3.1. Camera 1

Camera 1 was fixed at the top of a mast, which was slightly oscillating because of the wind even if the mast was stabilized by ropes. Indeed, a strong wind from the North-East is generally observed in this alley in the afternoon (mountain breeze). By averaging velocity results over 50 pairs of images, these oscillations were smoothed and the results remain coherent.

Fig. 3 gives an example of results obtained thanks to LSPIV measurements for camera 1. The x-coordinate corresponds to the East position in m whereas the y-coordinate corresponds to North position in m. Only the three last digits (Lambert 93 reference system) were kept for a better readability. Surface velocity vectors are represented on the left part of the figure (1) whereas surface velocity magnitudes ($U = \sqrt{U_x^2 + U_y^2}$ in m/s) are given on the right part of the figure (2). The "jet" forming at the entrance of the reservoir could be clearly observed thanks to the LSPIV measurements inducing a significant vorticity ($\Gamma = dU_x / dy - U_y / dx$) on the edges. As observed in Fig. 3 and Tab. 2, the maximum surface velocity of the jet is proportional to the input discharge although it is not as clear for larger discharges. Indeed, $V_{s,in} \approx$ 0.7, 1.2, and 1.4m/s, respectively for a input discharge $Q_{,in} \approx$

20, 40, and 70m^3/s. Some tentative measurements of the discharge (and velocity) were performed in the entrance canal using a Doppler profiler. But difficulties were encountered due to the eddies and maybe due to the large suspended sediment concentrations as well. Velocity estimates from the Doppler profiler were found 30% higher than from the LSPIV measurements.

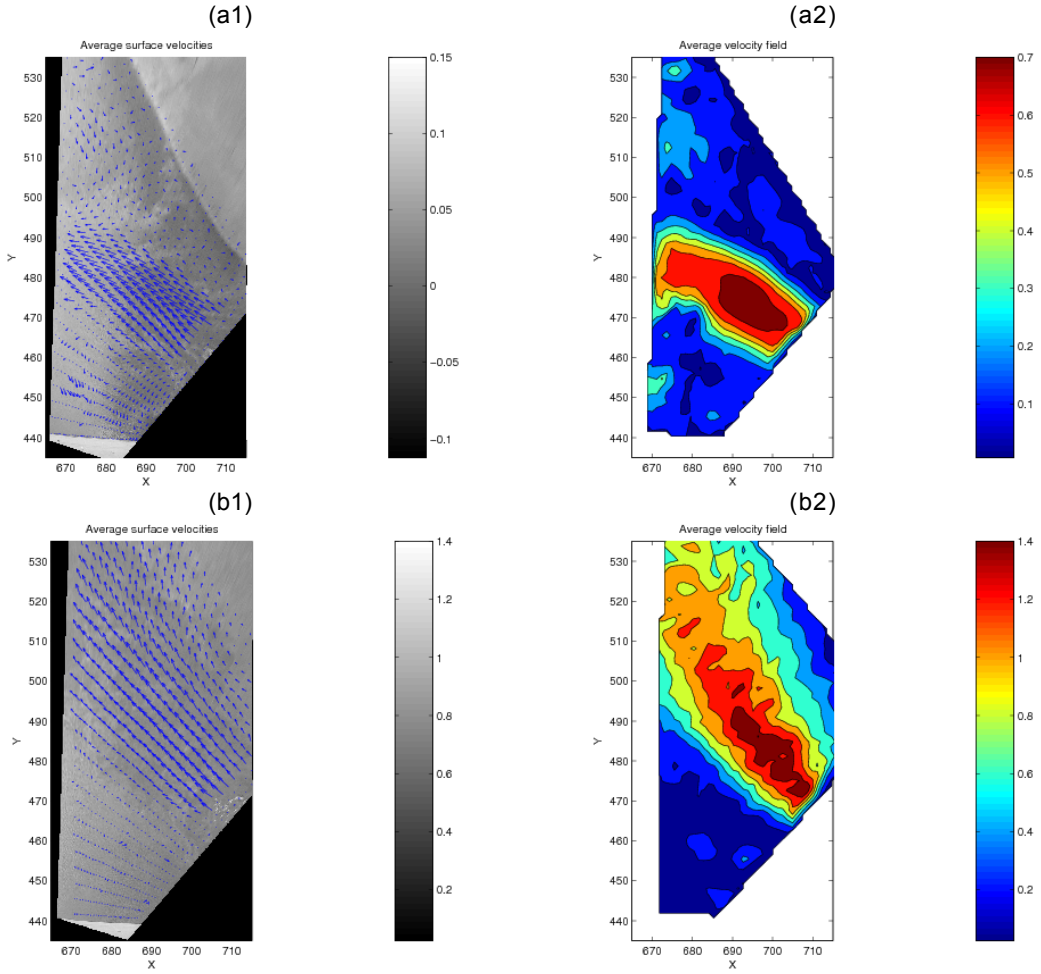

Figure 3 Surface velocity vector (1) and magnitude in m/s (2) measured from camera 1 on Sept. 25th at 9:25 (a, $z \approx 518.0$ m) and at 19:00 (b, $z \approx 520.9$ m).

Tab.2 summarizes the results obtained for the jet, i.e. direction and magnitude, together with the water level and water level variation. Apart for the sequence taken on the 26th at 14:55, for which the strong wind coming from the North-West may have modified the surface velocities, the direction of the jet is observed to be a function of the water level. It may be a consequence of the bathymetry influence on the water circulation due to the presence of the large deposits. However, it may also be only a coincidence as such a jet could be unstable. It should be noted that the velocity magnitudes given in Tab.2 are surface velocity magnitude. To obtained the depth-averaged velocity magnitude, a coefficient ($\alpha \approx 0.85$) should be added (Le Coz et al., 2010).

Table 2 Description of the jet observed at the entrance of the reservoir (jet direction angle from the x-axis).

Date	Time (UT +2)	Water level z (m)	dz/dt (10^{-4} m/s)	Jet direction (degrees)	Jet velocity (m/s)	Q_{in} (m^3/s)
25/09/2008	09:25	518.1m	+1	30	0.70	22
	15:35	517.9m	+1	30	1.30	41
	19:00	520.9m	-5	50	1.40	68
26/09/2008	09:35	518.3m	+2.5	35	1.20	41
	12:50	519.8 m	+1	40	1.20	60
	14:55	518.6 m	+1.5	15	1.40	60

3.2. Camera 2

From the camera 2, one could observe the main flow following the direction of the main channel (see Fig.2, where the velocities may reach 1m/s. Most often (see Fig. 4(a)), a significant recirculating flow was observed in the near field with velocity magnitudes of the same order of magnitude as the main flow (slightly smaller). This recirculating flow was also observed thanks to camera 1. A similar recirculation should have occurred on the right side of the jet and main flow. However, from the observation from camera 1, the magnitude may have been smaller. For the sequences taken in the afternoon of the 26th, the surface flow direction was nearly from East to West with no return flow (see Fig. 4(b)). This may be due to the strong wind that influenced significantly the surface velocities.

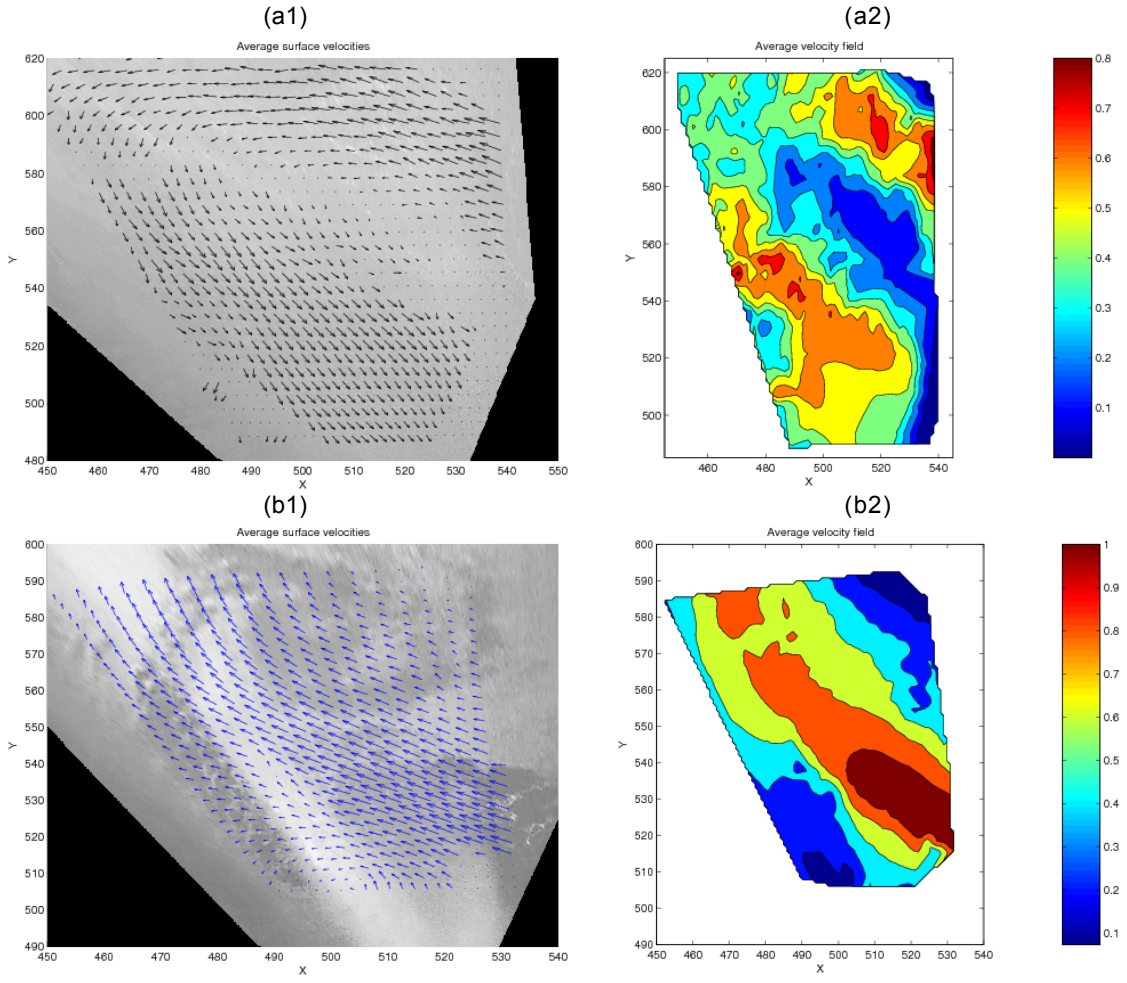

Figure 4 Surface velocity vector (1) and magnitude in m/s (2) measured from camera 2 on Sept. 25th at 14:10 (a, $z \approx$ 517.8 m) and on Sept. 26th at 11:45 (b, $z \approx$ 518.6 m)..

3.3. Camera 3

The position of the camera 3 was modified as it was disturbing the traffic around the reservoir during the event. The new position was not idealistic as the view scope was quite narrow and the quality of images was strongly affected by the sun reflections. In addition, no tracers could be observed. The bathymetry also strongly affected the direction and magnitude of the surface velocities. In particular, there is a clear deviation of the flow due to a small bar and due to the ramp (see Fig.5). Observed velocities were relatively high (V_s > 1.5 m/s) with the exception of the period when the water level was very high ($z \approx$ 520 m, same level as the circular spillway, $V_s \approx$ 0.5 m/s). An acceleration is observed close to the exit where the flow was often supercritical. It should be noted that most of the erosion observed during the flushing event occurred within this zone.

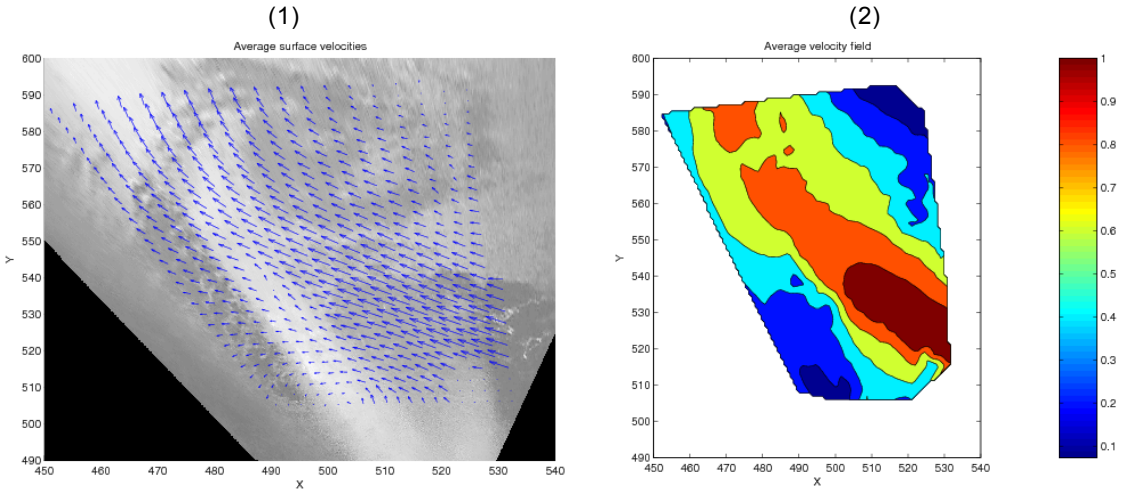

Figure 5 Surface velocity vector (1) and magnitude in m/s (2) measured from camera 3 on Sept. 25th at 10:25 ($z \approx 518.2$ m).

4. 2DH NUMERICAL MODELLING

Rubar20 (Paquier, 2010) and Telemac2D (EDF, 1998) are two dimensional in the horizontal (2DH) shallow water flow models. Telemac2D is based on a finite element approach with an unstructured mesh of triangles whereas Rubar20 is based on a finite volume approach with a structured mesh of quadrilaterals (see Fig.6). Both models were applied for the Longefan reservoir flushing event and compared to the LSPIV results.

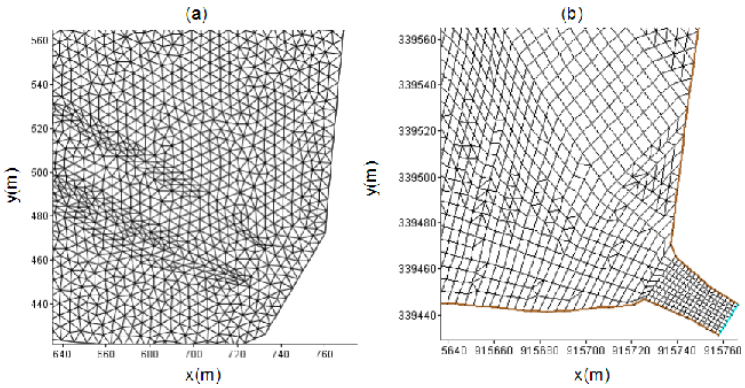

Figure 6 View of the mesh at the entrance of the reservoir for (a) Telema2D and (b) Rubar20 models (for the Telemac2D mesh, only the three last digits for the axis were displayed).

As it appeared that the entrance canal was of significant interest in the modelling of the "jet", it was added afterwards for the Rubar20 model (Fig.6(b)). First calculations with Rubar20 were achieved without entrance canal, similarly to the Telemac2D model. Another main difficulty for the modelling of the reservoir was the output boundary condition: the output discharge was estimated trough a gate hydraulic relationship, and the position of the gate was changed during the event (gate close on 25th from 5 to 6pm). This difficulty was tackled by adapting the gate relationship and by dividing the calculation in three steps (2nd step with the gate close).

In Fig.7, the direction angle (from the x-axis) of the jet at the entrance of the reservoir was plotted as a function of the water level using results from the LSPIV measurements and from the different models. For the Rubar20 (3) and Telemac2D cases, only the first part of the calculation is presented (before the gate was closed); that explains the lack of data from $z > 518.5$m. The models confirm the significant influence of the water level and so of the bathymetry on the direction of the jet as observed with LSPIV results (see also Tab.2). Both Rubar20 and Telemac2D models, for which the entrance canal was not modelled, yield very similar results in terms of direction. This direction angle is generally

overestimated and not as sensitive to the water level as shown with the LSPIV results. The boundary conditions appeared to significantly influence the direction of the jet. Indeed, the results obtained using Rubar20 with the entrance canal change drastically: the jet direction varies from 25 to 45 degrees depending on the water level. These results are in good correlation with the observations from LSPIV measurements. A third simulation was achieved with Rubar20 by adding the effect of a constant wind coming from North-West with a constant speed of 10m/s (surface forcing with the wind-related shear stress). Again, the results change drastically: the direction of the jet is decreasing with the water depth from 25 to 15 degrees when z_w < 518.5m. This simulation yet confirms the significant influence of the wind on the direction of the velocity as observed with LSPIV measurements on 25th at 14:55. Of course, because of the wind, surface velocity magnitude and direction may be significantly different from the depth-averaged velocity magnitude and direction as computed with 2DH models. This last simulation gives only an indication of the wind effects on the depth-averaged velocities.

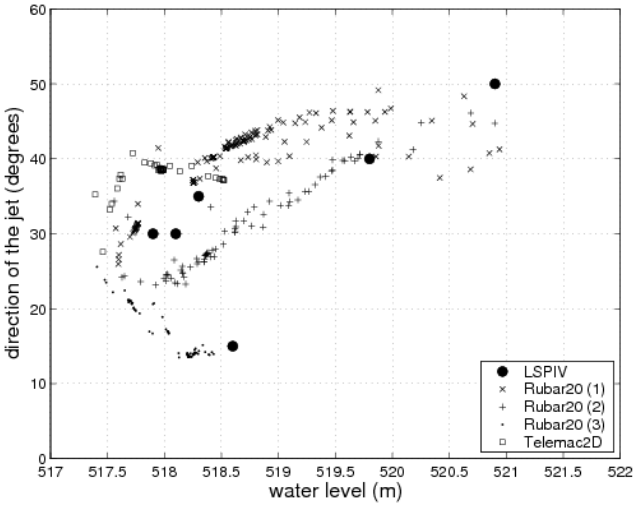

Figure 7 Direction of the jet observed at the entrance of the reservoir (jet direction angle from the x-axis) using LSPIV and modelled using Rubar20 without (1) and with (2 and 3) entrance canal and without (1and 2) or with (3) effect of the wind, and using Telemac2.

In term of velocities, the two numerical models are in good agreement with the LSPIV results. Depending on the water level, when $Q_{in} \approx$ 20m3/s, the velocity magnitude varies from 0.5 to 0.7m/s; when $Q_{in} \approx$ 40m3/s, it varies from 0.5 to 1m/s; when $Q_{in} \approx$ 70m3/s, it varies from 1 to 1.3m/s. In Fig. 8, the velocity field and water depths are presented for the simulation with Rubar20 including the entrance canal and without wind. Again, the general circulation observed thanks to the LSPIV measurement is well reproduced. In particular, the large recirculation cell on the left side of the main channel is correctly represented. However, the model does not show significant variations of the cell dynamics in time on the contrary to the observations. This may be due to the wind effects. Another point, the width of the main circulation appeared to be larger in the model compared to the observations by 50% approximately. For the downstream part of the reservoir, an acceleration of the flow is also observed with a similar order of magnitude for the velocities ($V_{max} \approx$ 2m/s, see also Fig. 5). The circulation around the small bar is however not very well reproduced.

5. CONCLUSION

LSPIV measurements were completed during a flushing event of a large reservoir using three cameras covering the main zones of interest (entrance, main channel and exit). The results obtained showed the significant effect of the bathymetry on the water circulation, in particular for the jet at the entrance of the reservoir. Indeed, the direction of the jet was observed nearly proportional to the water depth. The wind had also a significant influence on both surface and depth-averaged velocities.

Two 2DH hydrodynamic models (Rubar20 and Telemac2D) were applied to the system and presented similar results. The models confirmed the influence of the water level on the direction of the jet. The improvement of the boundary conditions, in particular the entrance canal but also the modelling of the downstream gate, appeared to be fundamental for the calculations. Final results are in good

agreement with the observations. The improvement of the velocity field computation is fundamental to better estimate fine sediment dynamics, especially for the source terms (erosion and deposition).

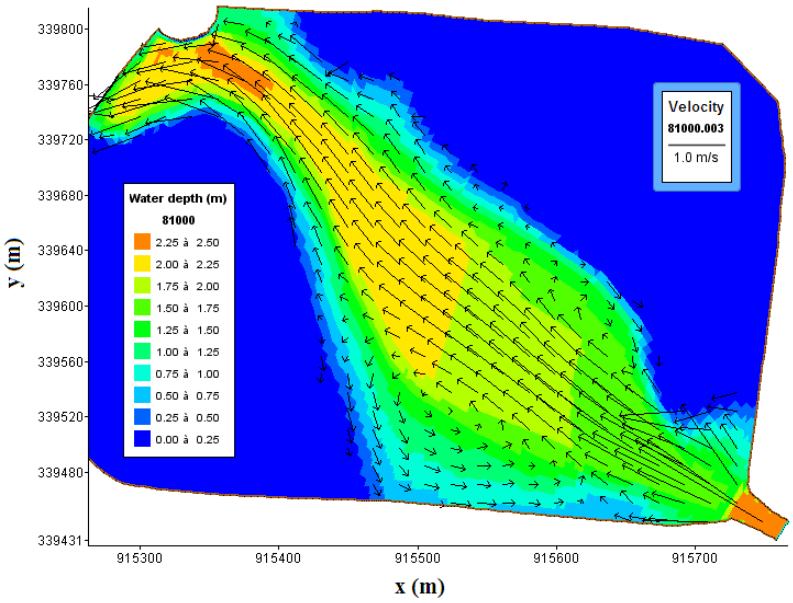

Figure 8 Velocity vector field and water depths obtained using Rubar20 (2) on 26th at 4am.

6. ACKNOWLEDGMENTS

We would like to thanks François Lauters and Eric Laperoussaz from EDF for providing all the complementary data.

7. REFERENCES

Camenen, B., Jodeau, M., and Le Coz, J. (2008). *Conceptual modelling of the sediment flux during a flushing event (Arc en Maurienne, France)*. In *Proc. 8th Int. Conf. on HydroScience and Eng.*, Nagoya, Japan. CD Rom.

EDF, L. (1998). *Modelling system Telemac*. EDF, Chatou, France.

Fujita, I., Muste, M., and Kruger, A. (1998). *Large-scale particle image velocimetry for flow analysis in hydraulic engineering applications*. J. Hydraulic Res., 36:397-414.

Jodeau, M., Hauet, A., Paquier, A., Le Coz, J., and Dramais, G. (2008). *Application and evaluation of LS-PIV technique for the monitoring of river surface velocities in high flow conditions*. Flow Measurement & Instrumentation, 19:117-127.

Le Coz, J., Hauet, A., Pierrefeu, G., Dramais, G., and Camenen, B. (2010). *Performance of image-based velocimetry (LSPIV) applied to flash-flood discharge measurements in Mediterranean rivers*. J. Hydrology, 394:42-52.

Morris, G. and Fan, J. (1998). *Reservoir Sedimentation Handbook: Design and management of dams, reservoirs, and watersheds for sustainable use*. McGraw-Hill Book Co., New York, USA.

Muste, M., Fujita, I., and Hauet, A. (2008). *Large-scale particle image velocimetry for measurements in riverine environments*. Water Resources Res., W00D19:14 p.

Paquier, A. (2010). *Logiciel Rubar20 Notice d'emploi*. Cemagref. (in French).

Yang, C. (2006). *Erosion and Sedimentation Manual*. U.S. Dep. of the Interior Bureau of Reclamation, Technical Service Center, Sedimentation and River Hydraulics Group, Denver, Colorado, USA.